Correlation between skin, bone, and cerebrospinal fluid layer thickness and optical coefficients measured by multidistance frequency-domain near-infrared spectroscopy in term and preterm infants

Anja Demel
Katharina Feilke
Martin Wolf
Christian F. Poets
Axel R. Franz

Correlation between skin, bone, and cerebrospinal fluid layer thickness and optical coefficients measured by multidistance frequency-domain near-infrared spectroscopy in term and preterm infants

Anja Demel,[a] Katharina Feilke,[a] Martin Wolf,[b] Christian F. Poets,[a] and Axel R. Franz[a,*]
[a]University Children's Hospital Tuebingen, Department of Neonatology, Calwerstr. 7, 72076 Tuebingen, Germany
[b]University Hospital Zurich, Biomedical Optics Research Laboratory, Division of Neonatology, Frauenklinikstrasse 10, 8091 Zürich, Switzerland

Abstract. Near-infrared spectroscopy (NIRS) is increasingly used in neonatal intensive care. We investigated the impact of skin, bone, and cerebrospinal fluid (CSF) layer thickness in term and preterm infants on absorption-(μ_a) and/or reduced scattering coefficients (μ_s') measured by multidistance frequency-domain (FD)-NIRS. Transcranial ultrasound was performed to measure the layer thicknesses. Correlations were only statistically significant for μ_a at 692 nm with bone thickness and μ_s' at 834 nm with skin thickness. There is no evidence that skin, bone, or CSF thickness have an important effect on μ_a and μ_s'. Layer thicknesses of skin, bone, and CSF in the range studied do not seem to affect cerebral oxygenation measurements by multidistance FD-NIRS significantly. © The Authors. Published by SPIE under a Creative Commons Attribution 3.0 Unported License. Distribution or reproduction of this work in whole or in part requires full attribution of the original publication, including its DOI. [DOI: 10.1117/1.JBO.19.1.017004]

1 Introduction

Near-infrared spectroscopy (NIRS) is a tool to evaluate tissue oxygenation noninvasively. As reported previously,[1–3] there are several instruments commercially available which use different techniques to measure tissue oxygenation, e.g., in the brain.

The NIRS quantifies the interaction of near-infrared photons with biological tissue, which can be described by two different properties: the absorption and reduced scattering coefficient (μ_a and μ_s').[4,5] Deoxygenated hemoglobin (HHb) and oxygenated hemoglobin (O$_2$Hb) are the most relevant chromophores absorbing light of the near-infrared spectrum and their concentrations can be calculated using the modified law of Lambert and Beer if the optical path length and geometrical factors are known.[6]

Unfortunately, standard NIRS devices currently are unable to measure path length, which is a function of the degree of scattering and absorption.[3,5] Hence, standard NIRS devices can only be used to assess changes in the concentrations rather than absolute concentrations of HHb and O$_2$Hb.

In contrast, frequency-domain NIRS (FD-NIRS) allows determining path length by measuring the phase shift of intensity modulated light after penetration of the tissues and hence enables one to measure the absorption coefficient (μ_a) and the reduced scattering coefficient (μ_s') based on the assumptions of homogeneity and semi-infinity.[4,5] Consequently, the FD-NIRS enables quantitative measurements of absolute concentrations of HHb, O$_2$Hb, total hemoglobin (tHb = HHb + O$_2$Hb) and tissue oxygen saturation (StO$_2$ = O$_2$Hb/tHb).

If the medium under investigation is not homogenous, then these absolute values may not be correct. For example, when measuring the neonatal head, the tissue is not homogenous, but has a layered structure of skin, bone, cerebrospinal fluid (CSF), and brain. This issue has been addressed in several studies using simulation, phantoms, and *in vivo* experiments. In simulations, it was shown for the neonatal head that a single light bundle is affected to between 8% and 23% by superficial tissue.[7] This result depends strongly on the assumptions made concerning the geometry of the neonatal head, such as the source-detector distances[8] and the shape and thickness of these layers.[7] An additional difficulty is that data on the thickness of the skull, skin, and CSF are not available for preterm infants. For the term neonates, we only found data on skin thickness.[9] For future simulations, it would be important to create reliable data on the thickness of these superficial tissues. In phantom studies, it was shown that by measuring at several different source detector distances (multidistance geometry), the effect of superficial tissue can be excluded mathematically.[10] *In vivo*, studies in adult subjects indicated that StO$_2$ values can be influenced by superficial tissues.[11,12] Again, no such studies are available in neonates yet, but according to the simulations, we expect that the influence of superficial tissue on the StO$_2$ value is much smaller in neonates or preterm infants compared to adults.

We aimed to measure the skin, bone, and CSF layer thickness in preterm infants and term neonates. The second aim was to investigate whether tissue thickness has an impact on absorption-(μ_a) or reduced scattering coefficient (μ_s') measured by multidistance FD-NIRS, to assess whether it should be taken into account whenever path length cannot be measured.

Table 1 Demographic characteristics of infants studied.

Clinical characteristics	Median/N	Range
Preterm/Term infants (n/n)	37/11	
Gender F/M (n/n)	28/20	
Gestational age at birth (weeks)	34 5/7	25 5/7 to 40 6/7
Postmenstrual age at measurement (weeks)	35 5/7	32 2/7 to 41 0/7
Postnatal age at measurement (days)	3	1 to 71
Birth weight (kg)	2.430	0.990–4.390
Head circumference (cm) at measurement	32.5	27.0–36.0
Weight at measurement (kg)	2.456	1.150 to 4.390
APGAR score at 5 min[a]	9	7 to 10
Umbilical artery pH	7.30	7.10–7.43

[a]The APGAR-score describes in brief the early postnatal adaptation of newborn infants by assessing appearance, pulse, grimace, activity, and respiration. Scores in the range encountered here are within the normal range, indicating that only healthy infants had been enrolled.

2 Subjects and Methods

The study was approved by the institutional ethics committee and written informed parental consent was obtained.

2.1 Patients

Term infants (11) and preterm infants (37) were studied at the neonatal intensive and high dependency care units of University Children's Hospital Tuebingen. Patient characteristics are shown in Table 1. Only infants who were hemodynamically stable, i.e., those with normal blood pressure and normal peripheral perfusion without circulatory support were included. Those with chromosomal or syndrome abnormalities were excluded.

2.2 NIRS Measurements

All measurements were performed while the infants slept in a supine position with their heads slightly elevated and turned to the side by <30 deg. The probe was positioned at the right temporo-parietal-region accurately in the middle between the tragus and the sagittal suture to avoid the sagittal sinus and the Sylvian fissure.

For each measurement, three separate recordings, each lasting at least 2 min, were performed with a sampling rate of 1 Hz. The optode was applied to the infant's skull with gentle pressure from the hand of the examiner. The optode was removed and repositioned for each recording.

Table 2 Skin, bone, and cerebrospinal fluid (CSF) thickness.

|	Minimum	Median	Maximum	Q1	Q3	CV (%)
Skin thickness (mm)	0.8	1.4	2.8	1.1	1.6	9 (0 to 39)
Bone thickness (mm)	0.7	2.2	4.6	1.1	2.8	9 (0 to 60)
CSF thickness (mm)	0.7	2.4	6.1	1.4	3.2	11 (0 to 77)
Combined thickness of all three layers (mm)	2.9	5.7	13.5	4.4	6.9	8 (1 to 57)

Note: Q1 = lower quartile; Q3 = upper quartile; CV = intra-subject coefficients of variation of three measurements of each layer thickness (a "most representative" measurement by clinical judgment, and two further measurements, each 8-mm right and left of the "most representative" one) determined in 41 (of 48) subjects and presented in (%) and as median and range.

**Table 3** Coefficients of absorption (μ_a) and reduced coefficients of scattering (μ'_s) at 692 and 834 nm.

	Minimum	Median	Maximum	Q1	Q3	Intra-subject CV (%)[a]	Inter-subject CV (%)
μ_a at 692 nm (1/cm)	0.035	0.096	0.183	0.068	0.110	6 (0 to 54)	34
μ_a at 834 nm (1/cm)	0.046	0.093	0.187	0.080	0.118	5 (0 to 92)	31
μ'_s at 692 nm (1/cm)	2.999	7.466	16.500	5.899	9.400	7 (0 to 80)	39
μ'_s at 834 nm (1/cm)	3.179	5.626	12.547	4.510	7.170	8 (0 to 66)	34

Note: Q1 = lower quartile; Q3 = upper quartile; CV = coefficient of variation.
[a]median (range).
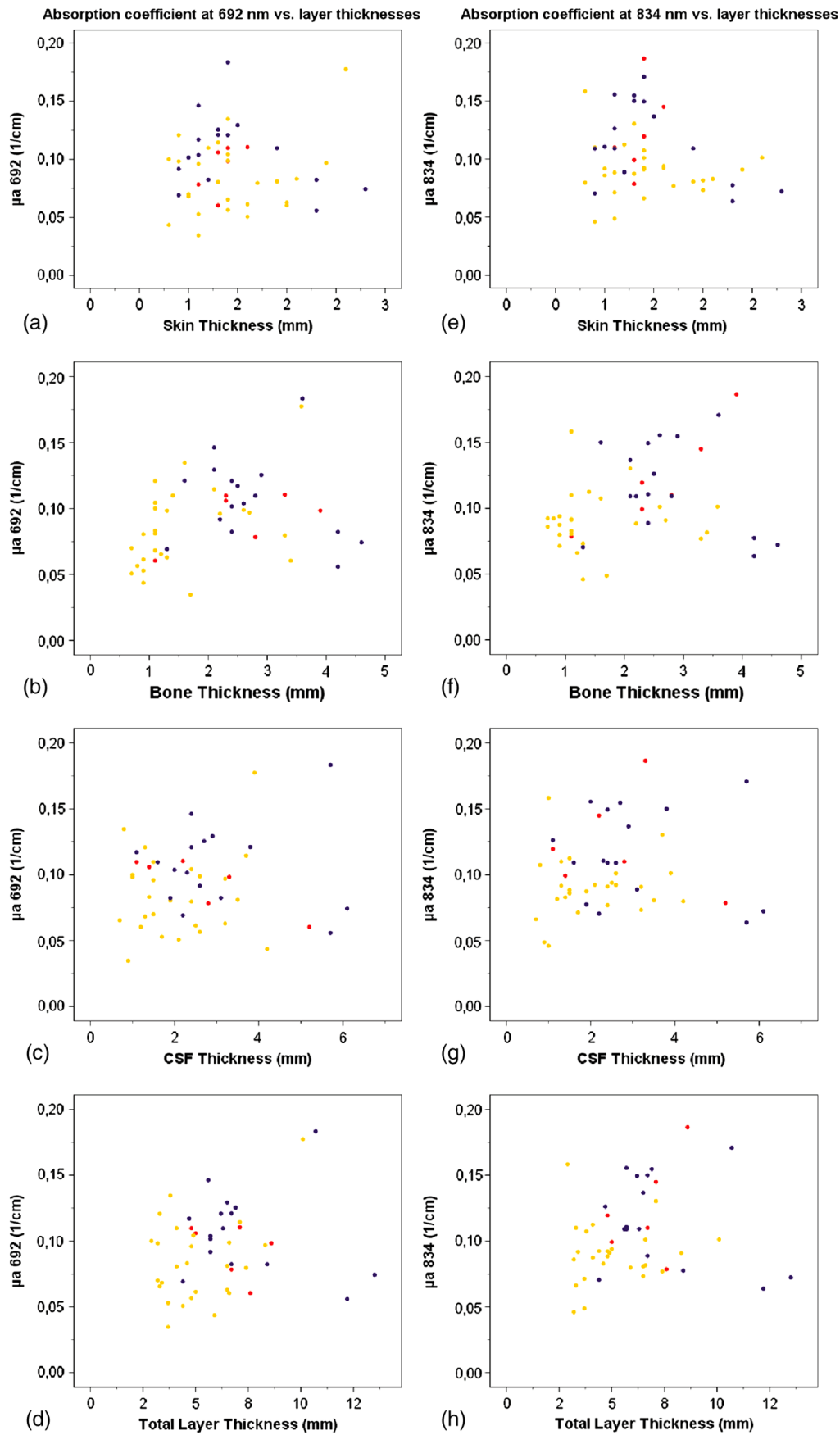
Fig. 1 Dot plots of absorption coefficients at 692 nm (a to d) and 834 nm (e to h) versus skin-, bone-, CSF-, and combined layer thickness. Color symbols show patients according to postmenstrual age at time of measurement: red = 32 to 35 weeks; yellow = 35 to 37 weeks; blue = 37 to 41 weeks.
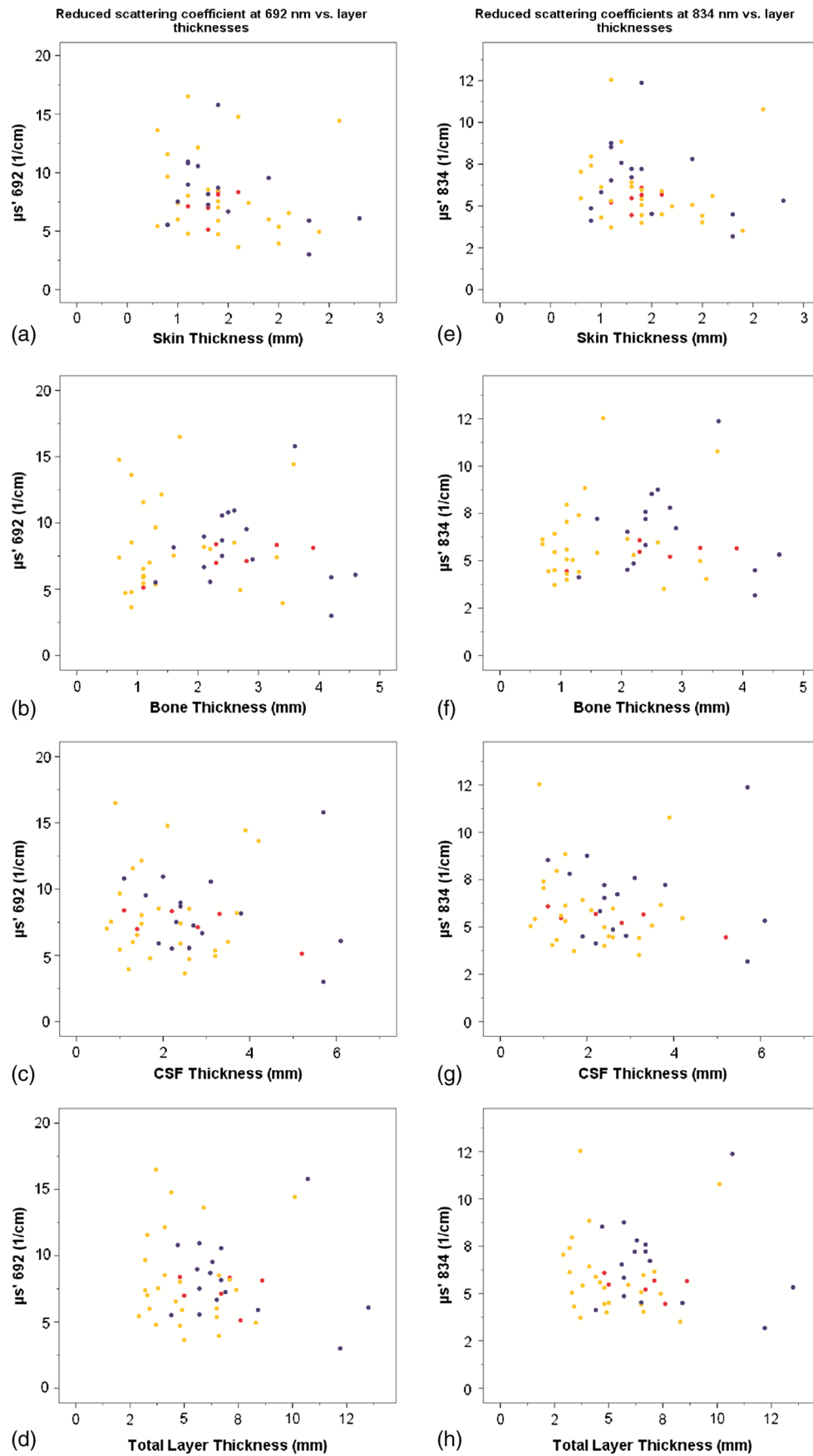
Fig. 2 Dot plots of reduced scattering coefficients at 692 nm (a to d) and 834 nm (e to h) versus skin-, bone-, CSF-, and combined layer thickness. Color symbols show patients according to postmenstrual age at time of measurement: red = 32 to 35 weeks; yellow = 35 to 37 weeks; blue = 37 to 41 weeks.

2.2.1 NIRS device

In this study, we used the ISS OxiplexTS (ISS Inc., Champaign, Illinois), an FD-NIRS. Each channel is equipped with eight infrared light sources at two different wavelengths (four emitting at 692 nm and four at 834 nm) each with four emitter–detector distances of 1.5, 2, 2.5, and 3 cm, resulting in penetration of biological tissues to 2 to 3 cm in depth (according to the manufacturer). To enable assessment of the path length by the phase-shift, the light intensity is modulated at a frequency of 110 MHz.

2.2.2 Calculation of absorption coefficients (μ_a) and reduced scattering coefficient (μ_s')

Light intensity and phase shift were recorded for each emitter–optode distance using the proprietary software package OxiTS, and μ_a and μ_s' calculated based on the slope of the respective regression lines at each wavelength using the diffusion equation for homogeneous, semi-infinite media as previously described.[4]

2.3 Cranial Ultrasound

The thickness of the skin, bone, and CSF layers was determined using cranial ultrasound (Aplio, Toshiba Medical Systems, Japan) applying a 7- to 14-MHz longitudinal transducer to exactly the same position of the head as the NIRS probe. The "most representative" thickness was determined for each tissue layer by best clinical estimate Fig. 4.

2.4 Arterial Oxygen Saturation

Arterial oxygen saturation as measured by pulse oximetry was continuously recorded using a Radical 7 pulse oximeter (Masimo Corp, Irvine, California).

3 Data Analyses

First, the median μ_s' and μ_a for every 2 min NIRS recording was determined. Thereafter, the median of the medians of all three 2 min recordings was calculated for each measurement. Furthermore, for arterial oxygen saturation the minimum value of all minimum measurements in each patient and the maximum of the corresponding maximums are reported.

To describe the intra-subject (i.e., spatial or probe-placement dependent) variability of μ_a and μ_s' of the three separate NIRS recordings in comparison to the inter-subject variability, the coefficients of variation (in %) for μ_a and μ_s' at both wave lengths were calculated as the ratio of the standard deviation divided by the arithmetic mean (1) of the three separate NIRS recordings within each subject, and (2) of the individual median values of all 48 subjects introduced into the correlation analyses.

To describe their variability, layer thicknesses were determined 8 mm to the right and 8 mm to the left of the "most representative" measurement, and the coefficient of variation was calculated for all three measurements in an individual patient. Because of limited quality of the ultrasound slides at larger distances to either side of the "most representative" measurement (due to the application of a linear ultrasound probe to the curved skull), it was not possible to systematically assess the variability of layer thicknesses over the maximum emitter–optode distance (30 mm) applied herein.

Coefficients μ_s' and μ_a were plotted against layer thicknesses for each wave length. Linear regressions and the nonparametric

Spearman rank regression coefficients were calculated to describe correlations of skin, bone, and CSF layer thicknesses with μ_s' and μ_a.

P values, indicating the probability for refusing the null hypothesis (that the Spearman rank correlation coefficients, *r*, is not different from 0) by mistake, of <0.05 were considered to indicate "significant" correlations.

SPSS 15 (for Windows, Chicago IL, USA) was used for data analysis.

4 Results

The measured thicknesses of skin, bone, and CSF are shown in Table 2, and absorption coefficients and reduced scattering coefficients at the two wave lengths are depicted in Table 3 along with intra- and inter-individual coefficients of variation. In Figs. 1(a)–1(h) and 2(a)–2(h), absorption coefficients and reduced scattering coefficients are plotted against thickness of skin, bone, CSF and combined thickness of all layers, respectively. Table 4 summarizes the Spearman coefficients of correlation.

There was no obvious relation between the thickness of these layers and μ_a or μ_s' at either wavelength in this patient population.

We performed similar analyses for the subgroups of term infants, preterm infants measured during their first 2 days of life, and older preterm infants—but again no consistent pattern of correlation was detected (data not shown).

Thickness of skin, bone, CSF and combined thickness of all three layers is plotted against postmenstrual age at the time of measurement in Figs. 3(a)–3(d). Furthermore, total hemoglobin content and regional cerebral oxygen saturation in the study population are plotted against postmenstrual age in Figs. 3(e) and 3(f).

Arterial oxygen saturation was stable and ≥91% in all infants throughout the measurements: 97 (91 to 99)%.

5 Discussion

The NIRS is increasingly used in neonatal intensive care. Instruments suitable and approved for continuous monitoring in this age group give readings on a measure of cerebral oxygenation based on several assumptions that may not hold true in

Table 4 Correlation between coefficients of absorption (μ_a) as well as reduced coefficients of scattering (μ_s') and thickness of skin, bone, and CSF, and combined thickness of all three layers.

		μ_a 692 nm	μ_a 834 nm	μ_s' 692 nm	μ_s' 834 nm
Skin thickness	*r*	−0.014	−0.138	−0.250	−0.290
	p	0.927	0.349	0.087	0.046
Bone thickness	*r*	0.310	0.209	0.100	0.141
	p	0.032	0.153	0.498	0.338
CSF thickness	*r*	−0.023	0.081	−0.143	−0.204
	p	0.875	0.586	0.322	0.165
Combined thickness	*r*	0.150	0.145	−0.092	−0.128
	p	0.309	0.325	0.535	0.387
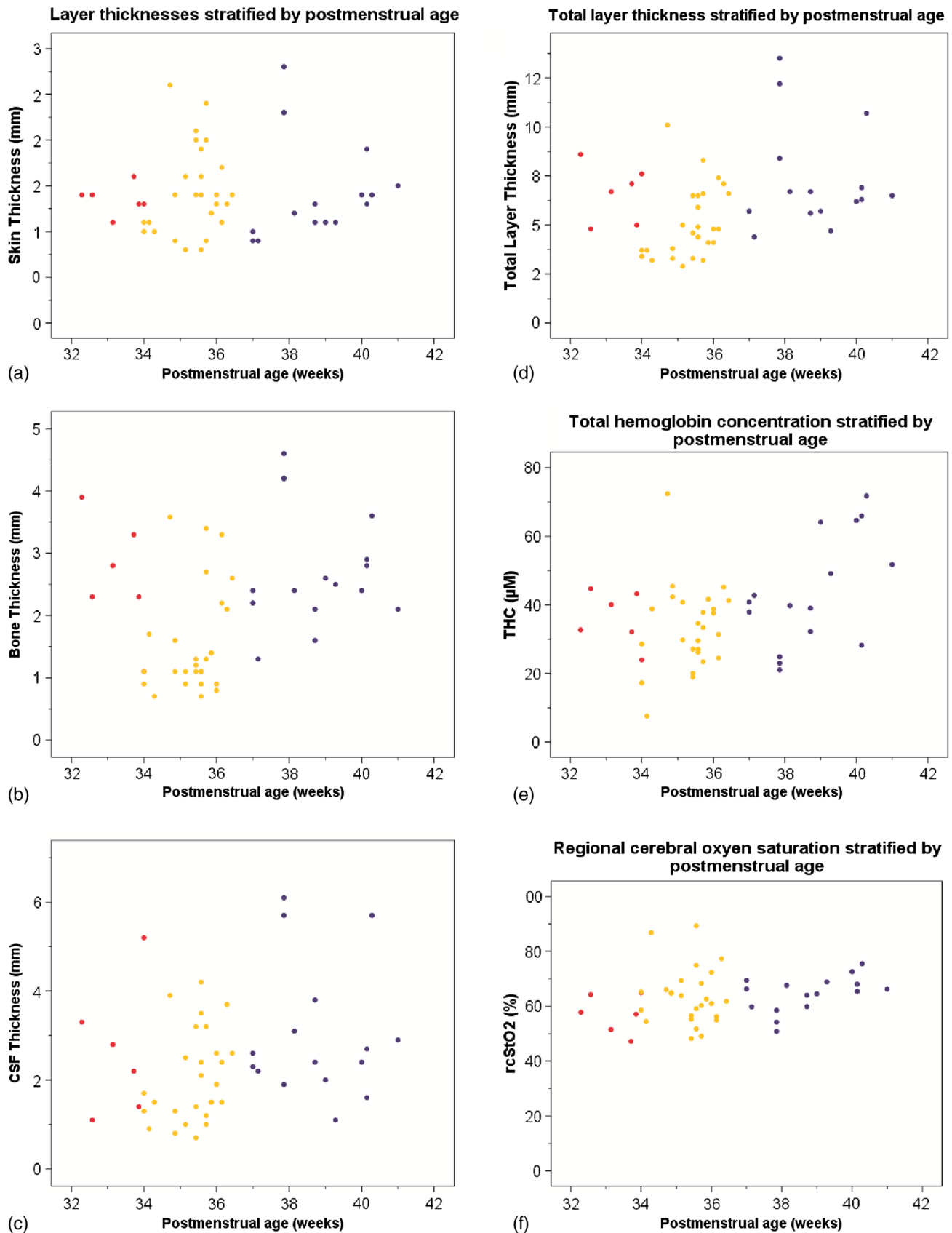
Fig. 3 Thickness of skin (a), bone (b), CSF (c), and combined layer thickness (d) for postmenstrual age at time of measurement are depicted. Total hemoglobin content (THC) (e) and regional cerebral oxygen saturation (f) in the study population according to postmenstrual age reflecting the previously described increase of regional cerebral oxygen saturation and THC with increasing postmenstrual age.

a given infant—and hence displayed values of cerebral oxygenation may not be appropriate in certain individuals.

Our study addressed the question whether the effects of the thickness of the layers skin, bone, and CSF consistently influences absolute μ_a or μ_s' based on the diffusion equation for homogeneous, semi-infinite media as measured by multidistance FD-NIRS in a mixed neonatal population. We hoped that integrating these layer thicknesses into algorithms that transform measured attenuation of near infrared light into measures of cerebral oxygenation would help to improve reliability of these readings. However, no such relationship was detected—apart from apparently "significant" correlations for μ_a at 692 nm with bone thickness and μ_s' at 834 nm with skin thickness, which we cautiously interpreted as chance findings given that (a) we performed 16 statistical tests without correction for multiple testing, (b) visual analyses of scatter plots did not support the findings of relevant correlations, and (c) no correlation was observed for μ_s' at 692 nm with skin thickness although the reduced scattering coefficients at the two wavelengths should be highly correlated themselves. Therefore, measures of cerebral oxygenation may not be consistently influenced by differences in these layer thicknesses within the range encountered in the described population at least if using multidistance FD-NIRS.

Our findings are in agreement with a previous report suggesting that, in a pig model, scalp, and skull thickness should have little impact on μ_a and μ_s'.[13] Furthermore, these results of *in vivo* measurements are in agreement with the *in vitro* study by Franceschini et al.,[10] showing that thin homogeneous layers above a semi-infinite block do not change μ_a and μ_s', at least as long as the layer is <0.4 cm thick.

We expected that at least the thickness of the CSF should have a consistent impact on μ_a and μ_s' because of potential "tunneling" of light in a clear fluid, but this could also not be detected in our population. There may be several explanations for not finding a major effect of CSF thickness on μ_a and μ_s': (1) Obviously, studying the thickness of the CSF as a single distance is a rather crude measure because this does not take into account that the "CSF space" anatomically consists of the cranial meninges of dura mater, arachnoid mater, and pia mater as well as CSF. It is not possible to discriminate those "sublayers" in detail by transcranial ultrasound, so that we accepted them as just one unit of measurement. This may be acceptable because Custo[14] demonstrated that the absorption of light by these meningeal membranes is very small. (2) Due to the gyri and sulci of the brain, CSF thickness is almost certainly variable over the four emitter–detector distances, whereas we only estimated a single value for CSF thickness in each patient. (3) Based on the work of Okada and Deply[15] it may be assumed that CSF (including arachnoid trabeculae) is a low scattering layer rather than a clear liquid. (4) Finally, other yet unknown and unmeasured covariables may have affected the measurements.

Hair follicles and hair, as well as skin color can absorb light at the wavelengths of interest for NIRS. Studies using a phantom showed that thick black hair, on its own, enhances absorption by up to 20%,[16] but no infant in our group had such hair or relevant skin pigmentation (all being of Caucasian origin), so that it is unlikely that these interfered with the measurements. Furthermore, care was taken to comb any existing newborn hair apart before placing the optode.

Similarly, van der Zee[17] demonstrated that white matter is more scattering than gray matter due to the high refractive index of myelin, but we were unable to take such influence
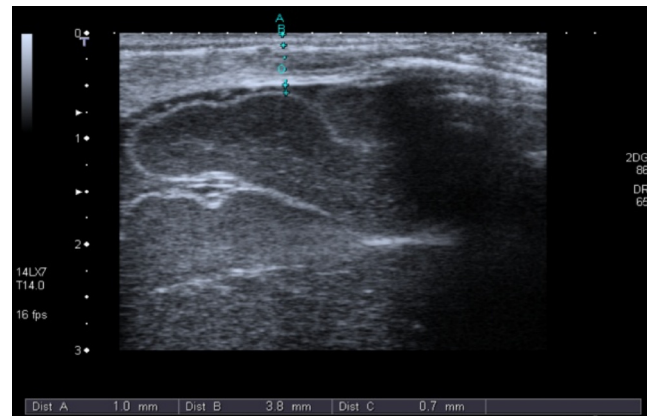

Fig. 4 Determination of tissue thickness by cranial ultrasound.

into account because myelination is hardly developed in newborn infants and assessment of gray matter thickness by ultrasound did not seem feasible.

We chose a mixed neonatal population, comprising term and preterm infants along with early and later postnatal measurements in the preterm population, to enable a good range of layer thicknesses, because the thickness of the layers is subject to developmental changes. Doing so meant that minor developmental changes in skin and brain water content were accepted, i.e., not taken into account for the analyses herein. It is noteworthy however, that even if the groups of term infants, preterm infants measured during their first 2 days of life, and older preterm infants were evaluated separately (to avoid variability introduced by different developmental stages), there was no consistent pattern of correlation between the optical parameters and extra-cerebral tissue layer thicknesses.

The position of the optode was chosen to enable measurements of layer thickness as depicted in Fig. 4 and to avoid that the falx cerebri or the sagittal sinus may influence NIRS readings,[18,19] given our relatively wide maximum emitter–optode distance of 30 mm.

The observed thicknesses of skin, bone, and CSF reported herein may be helpful for the creation of new head models to facilitate studies on NIRS in preterm and term infants. Although layer thicknesses were variable, intra-subject coefficients of variation of three measurements were <10% for all layers in the majority of individuals at least over a distance of 16 mm. It is a limitation that, due to the geometry of the ultrasound probe, we can neither provide data on layer thickness variability over the complete emitter–optode distance range of 30 mm, nor quantify exactly the layer thicknesses at the specific positions of emitters and optodes.

The lack of correlation between extra-cerebral layer thicknesses and the optical parameters μ_a and μ_s' may indicate that these layer thicknesses do not have a relevant impact on μ_a and μ_s' and consequently on measures of cerebral oxygenation. This conclusion is based on the assumption, that the inter-subject variability of μ_a and μ_s' resulting from variability of structural or physiological parameters was not large enough to overcome an existing underlying correlation between μ_a and μ_s' and extra-cerebral tissue thicknesses. If this assumption was incorrect, our conclusion would be invalid. As outlined above in support of our conclusion, we can specifically rule out major variability form clinically relevant anemia, hemodynamic disturbance, and diminished arterial oxygen saturation

(hence pathologically high or low cerebral concentrations of O_2Hb and HHb), ethnicity (hence relevant differences in skin and hair color and texture), and relevant white matter myelination (hence major variability in scattering properties of cerebral tissue) in our study population.

6 Conclusion

Skin-, bone-, and CSF-thickness within the range studied here did not correlate with and hence do not seem to have an effect on the absolute coefficients μ_a and μ_s' in term and preterm infants and may therefore be disregarded when calculating values for oxygenated and deoxygenated hemoglobin and measures of cerebral oxygenation, at least if measured by multidistance FD-NIRS.

References

1. G. Greisen, T. Leung, and M. Wolf, "Has the time come to use near-infrared spectroscopy as a routine clinical tool in preterm infants undergoing intensive care?," *Philos. Trans. A. Math. Phys. Eng. Sci.* **369**(1955), 4440–4451 (2011).
2. M. Wolf and G. Greisen, "Advances in near-infrared spectroscopy to study the brain of the preterm and term neonate," *Clin. Perinatol.* **36**(4), 807–834 (2009).
3. M. Wolf et al., "A review of near infrared spectroscopy for term and preterm newborns," *J. Near Infrared Spectrosc.* **20**, 43–55 (2012).
4. S. Fantini, M. A. Franceschini, and E. Gratton, "Semi-infinite-geometry boundary-problem for light migration in highly scattering media—a frequency-domain study in the diffusion-approximation," *J. Opt. Soc. Am. B* **11**(10), 2128–2138 (1994).
5. S. Fantini et al., "Non-invasive optical monitoring of the newborn piglet brain using continuous-wave and frequency-domain spectroscopy," *Phys. Med. Biol.* **44**(6), 1543–1563 (1999).
6. S. J. Matcher et al., "Performance comparison of several published tissue near-infrared spectroscopy algorithms," *Anal. Biochem.* **227**(1), 54–68 (1995).
7. E. Okada and D. T. Delpy, "The effect of overlying tissue on NIR light propagation in neonatal brain," *OSA TOPS on Adv. Opt. Imaging Photon Migr.* **2**, 338–343 (1996).
8. Y. Fukui, Y. Ajichi, and E. Okada, "Monte Carlo prediction of near-infrared light propagation in realistic adult and neonatal head models," *Appl. Opt.* **42**(16), 2881–2887 (2003).
9. B. A. Larsson et al., "Regional variations in skin perfusion and skin thickness may contribute to varying efficacy of topical, local anaesthetics in neonates," *Paediatr. Anaesth.* **6**(2), 107–110 (1996).
10. M. A. Franceschini et al., "Influence of a superficial layer in the quantitative spectroscopic study of strongly scattering media," *Appl. Opt.* **37**(31), 7447–7458 (1998).
11. K. Yoshitani et al., "Effects of hemoglobin concentration, skull thickness, and the area of the cerebrospinal fluid layer on near-infrared spectroscopy measurements," *Anesthesiology* **106**(3), 458–462 (2007).
12. S. N. Davie and H. P. Grocott, "Impact of extracranial contamination on regional cerebral oxygen saturation a comparison of three cerebral oximetry technologies," *Anesthesiology* **116**(4), 834–840 (2012).
13. M. Firbank et al., "Measurement of the optical properties of the skull in the wavelength range 650–950 nm," *Phys. Med. Biol.* **38**(4), 503–510 (1993a).
14. A. Custo et al., "Effective scattering coefficient of the cerebral spinal fluid in adult head models for diffuse optical imaging," *Appl. Opt.* **45**(19), 4747–4755 (2006).
15. E. Okada and D.T. Delpy, "Near-infrared light propagation in an adult head model. I. modeling of low-level scattering in the cerebrospinal fluid layer," *Appl. Opt.* **42**(16), 2906–2914 (2003).
16. M. Keel et al., "Regional differences of cerebral hemoglobin concentration in preterm infants measured by near infrared spectrophotometry," *Technol. Health Care* **7**(1), 63–73 (1999).
17. P. van der Zee et al., "Experimentally measured optical pathlengths for the adult head, calf and forearm and the head of the newborn infant as a function of inter optode spacing," *Adv. Exp. Med. Biol.* **316**, 143–153 (1992).
18. M. Ferrari, L. Mottola, and V. Quaresima, "Principles, techniques, and limitations of near infrared spectroscopy," *Can. J. Appl. Physiol.* **29**(4), 463–487 (2004).
19. M. Dujovny et al., "Use of cerebral oximetry to monitor brain oxygenation reserves for skull base surgery," *Skull Base Surg.* **4**(3), 117–121 (1994).

Biographies of the authors are not available.